IECON2015-Yokohama
November 9-12, 2015

Modeling and Analysis of Core Losses of an IPM Machine for Online Estimation Purposes

Shamsuddeen Nalakath, Matthias Preindl, Yinye Yang, Berker Bilgin, Bing Cheng, and Ali Emadi
Department of Electrical and Computer Engineering
McMaster University, Hamilton, Ontario, Canada

***Abstract*—Online estimation of losses is important to improve control, operation and monitoring of electrical machines. This paper focuses on investigation of iron losses using a magnetic circuit model for its accuracy and adaptability to online estimation purposes. A customized magnetic circuit of an IPM machine is proposed that captures slotting, non linearity, cross saturation and localized effect of flux bridges. A technique is presented to compute the alternating stator and rotor flux from the static magnetic circuit. The required computations are reduced introducing pseudo mmf sources that avoid solving magnetic circuit at several rotational steps. The stator and rotor core losses are found corresponding to each harmonic component of alternating flux density. The results are validated with Finite Element analysis with good correlation.**

I. Introduction

The high speed electric machines with reduction gears have gained interest in transportation application as they are lighter and smaller as compared to direct driven low speed electrical machines of the same power. The losses which are functions of frequency are the prevailing concerns while adopting them in the indirect drive applications [1]-[5]. The core and AC copper losses are the main loss components which are depended on frequency. The latter one is due to eddy current induced in the conductor by skin and proximity effects. They can be estimated with analytical models [1]-[3]. On the other hand, it is difficult to find a closed form expression for the core loss as the flux density is distributed heterogeneously in electrical machines [4][5].

The prediction of core loss with the help of magnetic circuit (MC) is a method well used in rapid design process [4]-[6]. The magnetic circuit predicts the average distribution of flux density across a region. This information is used to calculate the core loss. However, building a magnetic circuit is a challenge for the machines like interior permanent magnet (IPM) [6]-[8]. The effects of slotting, non linearity, cross saturation and flux bridges are the main challenges. The lack of careful modeling of these effects results in deviations from the actual flux densities. Unlike surface permanent magnet (SPM) machines, the rotor core loss is not negligible for IPMs as the core directly faces the air gap. The flux in the rotor core alternates due to slotting and PWM harmonics [7][8]. A detailed air gap circuit model is required and the circuit has to be reconnected at each rotor positions to capture these harmonics [7][8].

Once the flux densities of each magnetic circuit elements are known, then the Steinmetz's equation can be used to find the core loss. If the flux density is not sinusoidal, then the core loss corresponds to each harmonic flux density is added up to get the total core loss. The coefficients of Steinmetz equation are treated generally as constants. Actually, they vary with flux density and frequency [9][10]. These coefficients are extracted from manufacture's loss data for the given material. The modified Steinmetz equations are used to account for PWM and arbitrary waveforms [11][12]. The rotational nature of the flux vector at some regions of the core creates some additional core loss [13][14]. The loci of the flux rotation helps to quantify this loss.

The application of MC for online estimation of the core loss is investigated in this paper. An exclusive MC which captures nonlinear behavior of the core, cross saturation, slotting, and localized effect of flux bridges is proposed. The MC is solved with the help of MATLAB nonlinear solver 'fsolve'. The results are used to find the flux variation corresponding to all the time steps in an electrical cycle. An exclusive circuit which has only harmonic mmf sources is proposed to find the variation in rotor flux density. The Steinmetz equation is used to find the core loss at different harmonics. The results are compared with FE analysis at different load currents and excitation angles (field weakening).

II. Online Core Loss Estimation Scheme

There are different techniques available in literature related to online estimation of core loss. The total core loss at any operating condition is expressed in terms of the rated core loss, ratio of operating and rated flux and frequency for a self excited induction generator [15]. The total core loss is modeled as resistive component and it is corrected with the help of adaptive techniques for an induction motor [16]. The similar techniques can also be applied to IPM machines. However, the localized behavior due to flux bridges, cross saturation and rotor core loss at slot harmonic orders cannot be captured. Also, if the estimated core loss is used for temperature estimation, then the distributed core loss would give better estimation.

In this paper MC is chosen to estimate the core loss. The block diagram of the scheme is presented in Fig. 1. Online information of current and excitation (FW) angle are fed to the MC model. Then the model estimates the flux densities of all the regions in the stator and rotor cores. These results and operating frequency are then fed to the core loss model which estimates the core losses in stator and rotor at the fundamental and the harmonic frequencies.

978-1-4799-1762-4/15/$31.00 ©2015 IEEE

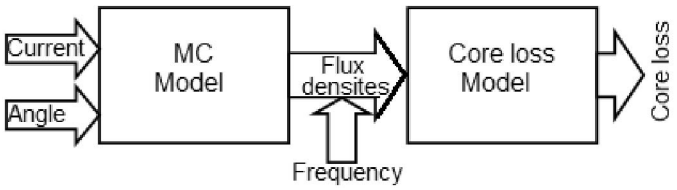

Fig. 1: Online core loss estimation scheme.

III. Magnetic Circuit Modeling

The first step in building a magnetic circuit model is discretizing the core into several regions. The area which has the same flux density is considered as a region. The regions are then modeled as reluctance elements. These elements are interconnected based on the flux path. The static FE analysis is carried out in order to understand the flux distribution in the core. Figure 2 shows the discretization based on FE results of the IPM machine considered in this paper. The rotor front island, back island and the magnet are divided into three regions. The rotor island region has the flux in both the radial and the tangential directions which capture cross saturation. The tooth is divided into two regions. The hat, slot and slot opening are single regions. The stator back iron is divided into three regions.

The air gap spanning one slot pitch is discretized into three regions. They are the regions above slot opening, hat, and tooth stalk as shown in Fig. 3. The reluctance elements of these three regions are individually connected to the elements corresponding to their bottom regions in the stator. On the rotor side, these three elements are shorted and connected to the front rotor island. The air gap elements along with the elements of hat, slot opening, and tooth stalk help to model the slotting. Its accuracy is very important in predicting rotor core loss.

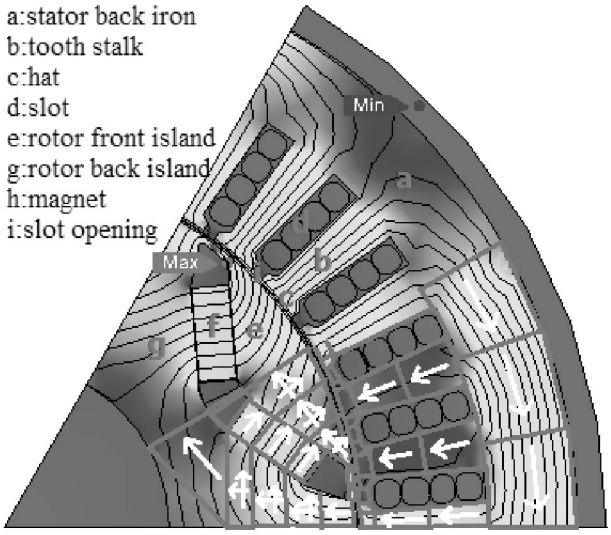

Fig. 2: The discretization of stator and rotor cores.

The MC is modeled for one pole pair and the end terminals from one side are connected to other side to form a continuous circuit as shown in Fig. 4. The stator mmf sources are connected in between stator back iron and tooth stalk elements. The mmf value corresponding to one tooth is found by averaging mmf over a slot pitch. The magnet source is divided into three regions. This helps to capture local effects due to flux bridges. There are flux bridges between the magnets and one near the air gap. The latter one is divided into two to capture its effect on the air gap field.

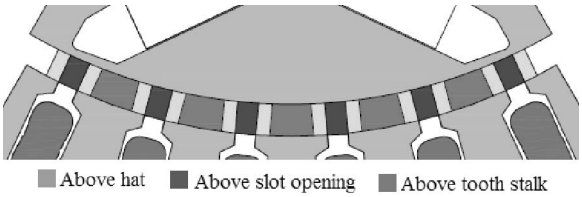

Fig. 3: The discretization of air gap.

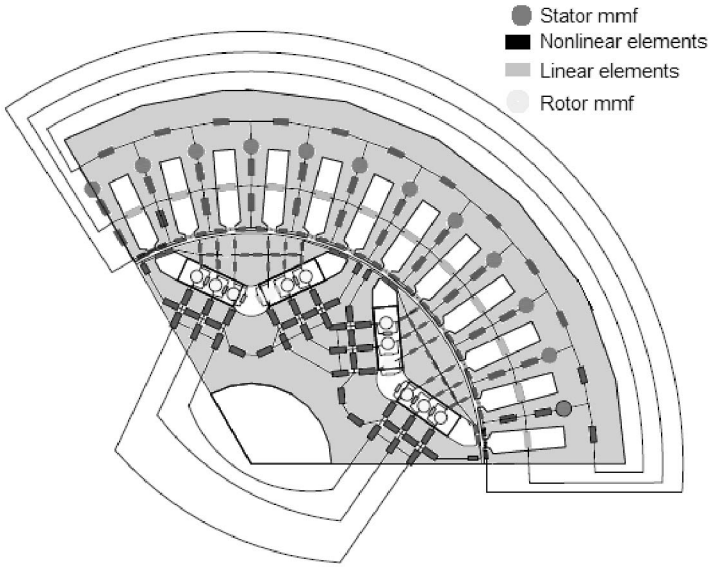

Fig. 4: The magnetic circuit model.

The steel regions are modeled as 174 nonlinear elements. There are 120 linear elements, 24 mmf sources and total 54 flux loops. The matrix equation of the circuit is

$$[M]_{54\times1} = [R]_{54\times54}\ [\phi]_{54\times1} \tag{1}$$

where M is mmf vector, R is reluctance matrix and ϕ is loop flux vector. The flux density distribution in the alternate quarters of the model is similar, as shown in Fig. 2. Hence the elements in the matrix are identical and this helps in reducing the solving time.

The soft magnetic material used for the IPM considered in this paper is 50CS350 (China Steel). The B-H curve of the steel is shown in Fig. 5. The reference IPM machine has 36 slots, 6 poles, and 48 turns per phase. The machine is rated for 10KW at 8000 rpm.

The MC model is solved in MATLAB nonlinear solver 'fslove'. The air gap flux density profile at 50Hz, 50 Ap phase current and different current excitation angles (angel from q-axis) 0^o, 30^o, and 60^o are respectively shown in Fig. 6, 7 and 8. In all the three cases, the results from the MC closely match

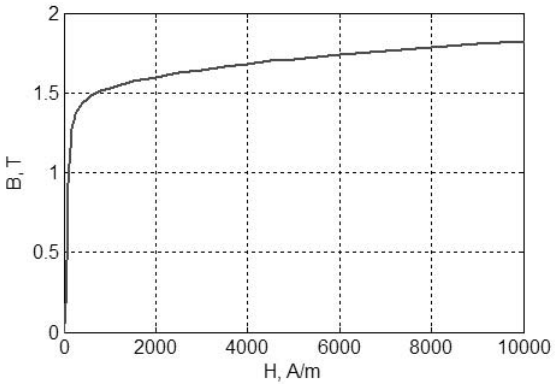

Fig. 5: B-H curve of 50CS350.

with the FE results. The per unit values of flux density in this paper has the base of 1.1 T. It is challenging to accurately predict the flux density around the flux bridges due to strong saturation nonlinearity. However, the introduced two elements as mentioned in the previous section significantly improved the results as shown between 5^o-15^o and 45^o-55^o mechanical degrees.

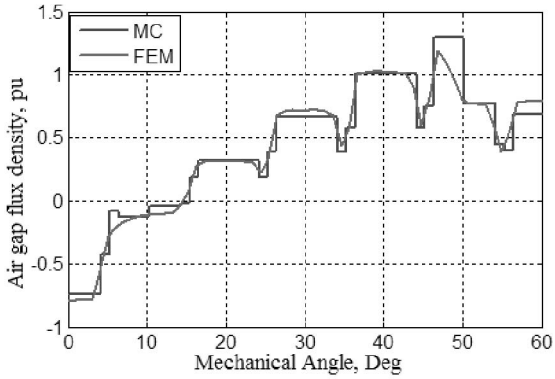

Fig. 6: Air gap flux density at 0^o current excitation angle.

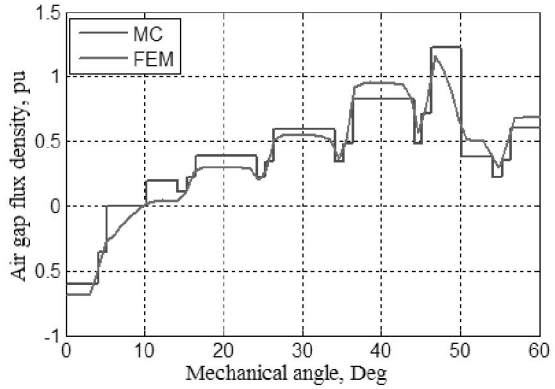

Fig. 7: Air gap flux density at 30^o current excitation angle.

The solution of the magnetic circuit gives static values of loop flux densities for a given operating point. The generation of alternating flux densities and estimation of core loss come under post processing.

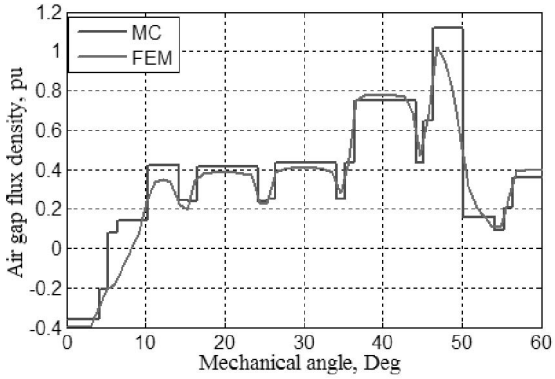

Fig. 8: Air gap flux density at 60^o current excitation angle.

IV. Alternating Stator Flux Density

The flux in the stator rotates at the excitation frequency. Therefore each stator region experiences alternating flux. The stator elements, which are considered for core loss estimation, are grouped as upper tooth that faces the air gap, bottom tooth and stator back iron. The elements of hat region are not considered as they are small. The flux in one element of a group is the same as the flux in its preceding or succeeding element at the previous rotational step depending on the direction of rotation of flux. This is mathematically expressed as

$$\phi_{(n,k+1)} = \phi_{(n-1,k)} \tag{2}$$

where, n is the element index and k is rotational step index. This fact is used to obtain the alternating flux densities in the stator elements. The flux densities of all the elements in a group from static solution of MC together represent the alternating flux density corresponds to one electrical cycle for an element.

There are 12 slots per pole pair for the reference IPM, which provide 12 flux density points as shown as step profile in Fig. 9, Fig. 10 and Fig. 11 for top tooth, bottom tooth and stator back iron, respectively. The step profile results in unreal harmonics. Therefore, an interpolation connecting 12 points is carried out for all the groups. The interpolated profiles show good correlation with FE results. The FE results are average flux densities over the discretized regions at each rotational steps.

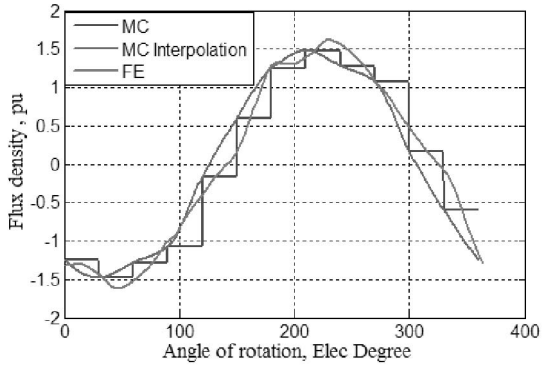

Fig. 9: Alternating flux density in the top tooth element.

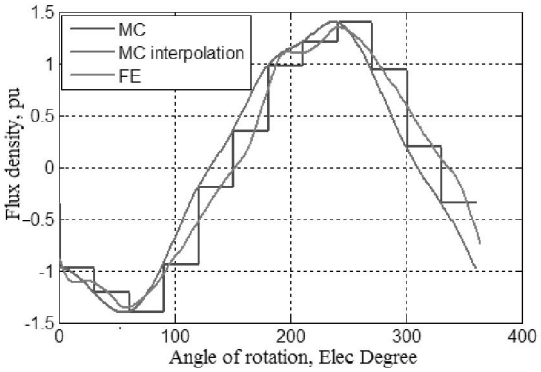

Fig. 10: Alternating flux density in the bottom tooth element.

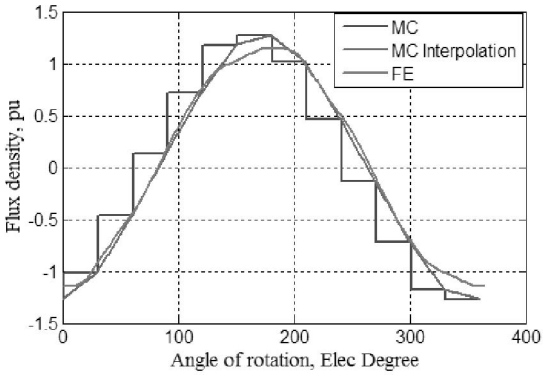

Fig. 11: Alternating flux density in the stator back iron element.

The alternating flux density profiles shown in Fig. 9, 10 and 11 are not sinusoidal. Therefore, the core loss are found separately for each harmonics. The harmonic components of flux densities along with their corresponding values form FE are shown in Fig. 12, 13 and 14. The values show good correlation with FE results. The harmonics at the order of 6 are negligible, but they are the main components in the rotor.

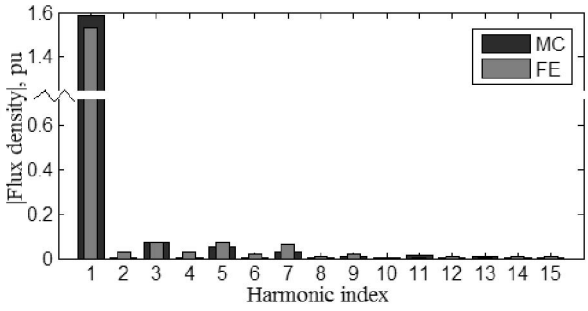

Fig. 12: Fourier decomposition of flux density in the top tooth element.

V. Alternating Rotor Flux Density

The rotor rotates synchronously with the stator field. Hence the rotor magnetic field is stationary as observed from the rotor reference frame.. However, the slotting, distribution, non sinusoidal excitation and PWM could cause higher order alternating fields in the rotor. These result in substantial

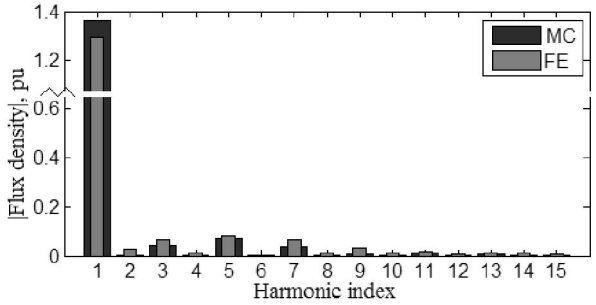

Fig. 13: Fourier decomposition of flux density in the bottom tooth element.

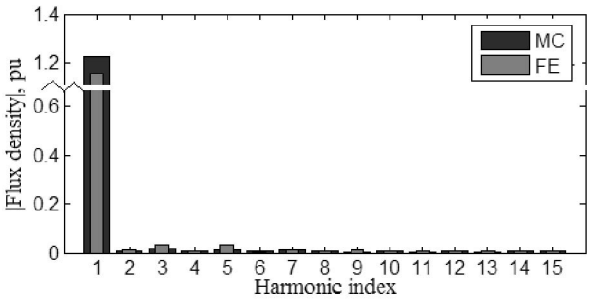

Fig. 14: Fourier decomposition of flux density in the stator back iron element.

core and permanent magnet losses. It is very challenging to obtain these harmonics with a MC[7][8]. This paper proposes a simple and a faster method. It provides magnetic field density of any element for any harmonic order by solving an exclusive magnetic circuit (ExMC). The ExMC is similar to the actual MC as shown in Fig. 15. However, the mmf sources are shorted and introduced pseudo mmf sources in the air gap having harmonic orders. The values of pseudo mmf sources are essentially air gap mmf harmonics found by Fourier decomposition.

Fig. 15: Exclusive slot harmonic circuit.

The sinusoidal three phase excitation without PWM is applied to FEM model and the analysis shows that the dominant

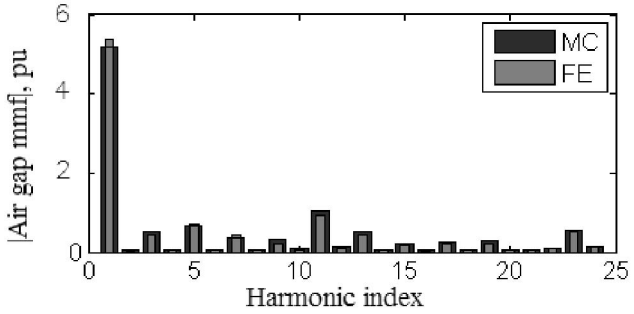

Fig. 16: Fourier decomposition of air gap mmf.

rotor harmonics are from slotting, which are at the orders of 6. The values of these harmonics for ExMC are found from the actual MC. The Fourier decomposition of air gap mmf at 300Ap phase current and 30^o excitation angle is shown in Fig. 16. The base value of per unit mmf is 100 A. The ExMC is solved for each slot harmonics. The ExMC is approximated as linear as the flux density is low when excited with harmonic mmfs. The flux density values from ExMC and FEM at right, center and left regions of rotor front island are shown in Fig. 17, 18 and 19 respectively. The ExMC results are geometric sum of the flux densities in radial and tangential elements.

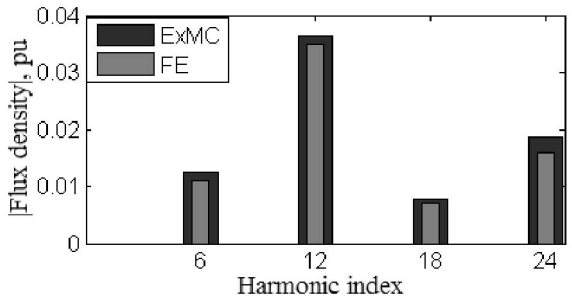

Fig. 17: Fourier decomposition of right region of front island.

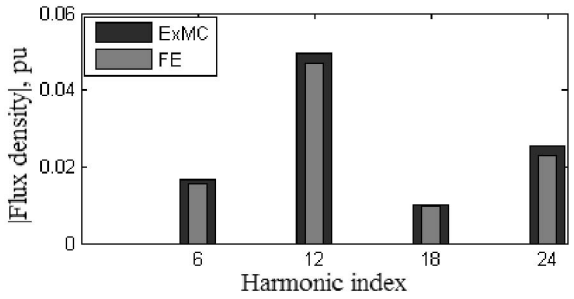

Fig. 18: Fourier decomposition of center region front island.

VI. Core Loss

The Steinmetzs equation is used to find the core loss. The loss contributed by total n harmonics and k elements are

$$P_{core} = \Sigma_{ki=1}^{k} \Sigma_{ni=1}^{n} \left(kh_{ni} {B_{ni,ki}}^{1.6} fn + ke_{ni} {B_{ni,ki}}^{2} (fn)^2 \right) \quad (3)$$

where kh and ke are hysteresis and eddy current coefficients, ki and ni are element and harmonic indexes.

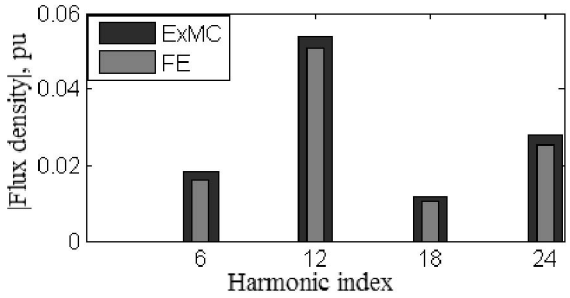

Fig. 19: Fourier decomposition of left region of front island.

The values of kh and ke are found from manufacture's loss data. The loss data for different frequencies and flux densities for 50CS350 steel is shown in Fig. 20. The curve fitting coefficients for each curve corresponding to a flux density are essentially the core loss coefficients. The coefficients vs flux density are plotted in Fig. 22 and Fig. 21.

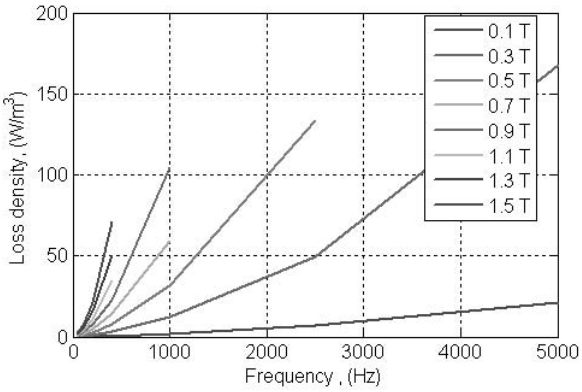

Fig. 20: Manufacture's core loss data for 50CS350.

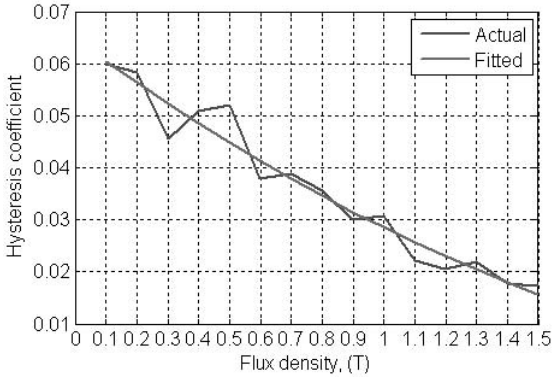

Fig. 21: Hysteresis loss coefficient.

The core loss results from MC are compared with FE at several operating points. The difference is in the range of 5%-20%. The per unit values of rotor and stator core losses at 300Hz, 300Ap (causes high saturation) and 30^o current excitation angle with the base of 10 W are shown in Fig. 23 and 24 respectively.

The computation time took to solve the nonlinear circuit is 4s in Intel Core i7-4770 CPU @3.4 GHz, 32 GB RAM computer. Whereas, solving magneto static model by the

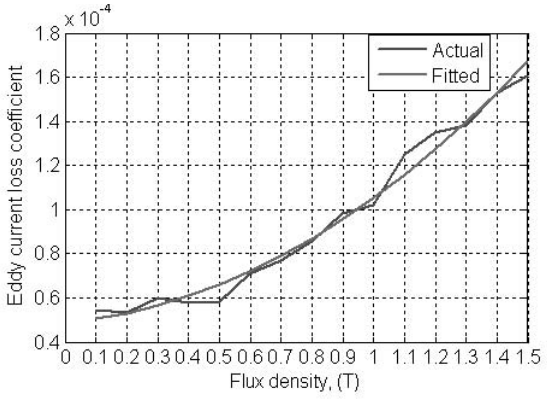

Fig. 22: Eddy current loss coefficient.

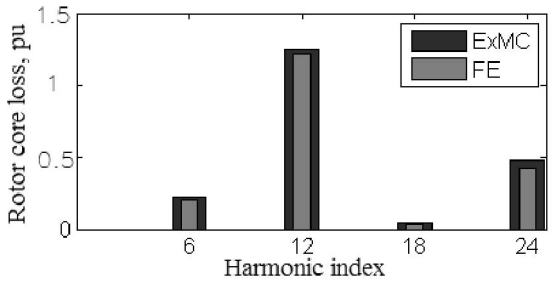

Fig. 23: Rotor core loss.

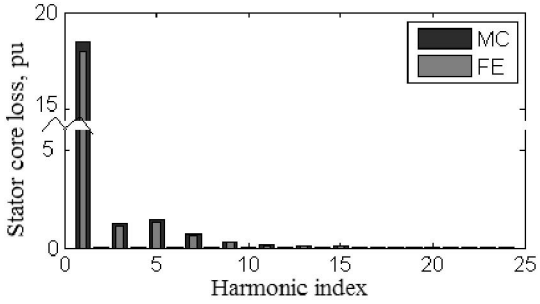

Fig. 24: Stator core loss.

commercial FE software, JMAG, takes 240s in the same computer. The reduction of the computation time to implement in an embedded platform is the key focus for the future work.

VII. Conclusion

This paper presents a customized magnetic circuit which captures detailed effects like cross saturation, slotting and local effect due to flux bridges for an IPM machine. The simple and faster methods to obtain the alternating flux density in stator and rotor regions are presented. The alternating flux density profile and their harmonic components showed good correlation with the FE results. The stator and rotor core losses are estimated for each harmonic components. The core loss results for a specific operating condition are presented and they are in good match with the FE results. Although, the total computation time is 60 times lesser than FE, the time required to solve in embedded platform might take longer. The reduction of computation time is going to be the key focus of the future work.

VIII. Acknowledgment

This research was undertaken, in part, thanks to funding from the Canada Excellence Research Chairs Program and the Natural Sciences and Engineering Research Council of Canada (NSERC) Automotive Partnership Canada (APC) Initiative. The authors also gratefully acknowledge Powersys solutions for their support with JMAG software in this research.

References

[1] C.R. Sullivan, "Computationally efficient winding loss calculation with multiple windings, arbitrary waveforms, and two-dimensional or three-dimensional field geometry," *IEEE Trans. Power Electron.*, vol.16, no.1, pp.142,150, Jan 2001.

[2] S. Sudhoff, "AC conductor losses," in *Power Magnetic Devices:A Multi-Objective Design Approach*, WILEY-IEEE PRESS,2014.

[3] L.J. Wu et al., "Analytical Model of Eddy Current Loss in Windings of Permanent-Magnet Machines Accounting for Load," *IEEE Trans. Magn.,* vol.48, no.7, pp.2138,2151, July 2012.

[4] A.S. Thomas et al.,"Proximity Loss Study In High Speed Flux-Switching Permanent Magnet Machine," *IEEE Trans. Magn.,* vol.45, no.10, pp.4748,4751, Oct. 2009.

[5] J.K Tangudu et al., "Lumped parameter magnetic circuit model for fractional-slot concentrated-winding interior permanent magnet machines," in Energy Conversion Congress and Exposition, 2009. ECCE 2009. IEEE, doi:10.1109/ECCE.2009.5316069.

[6] Y. Kano et al., "Simple nonlinear magnetic analysis for permanent-magnet motors,"*IEEE Trans. Ind. Electron.*, vol.41, no.5, pp.1205,1214, Sept.-Oct. 2005.

[7] E.C. Lovelace et al., "A saturating lumped parameter model for an interior PM synchronous machine," *IEEE Trans. Ind. Electron.*, vol. 38, no. 3, MAY/JUNE 2002.

[8] Seok-Hee Han et al., "A Magnetic Circuit Model for an IPM Synchronous Machine Incorporating Moving Airgap and Cross-Coupled Saturation Effects," in Electric Machines Drives Conference, 2007. IEMDC '07. IEEE International, doi:doi: 10.1109/IEMDC.2007.383546.

[9] J.K. Tangudu et al., "Core loss prediction using magnetic circuit model for fractional-slot concentrated-winding interior permanent magnet machines," in Energy Conversion Congress and Exposition, 2010. ECCE 2010. IEEE, doi:10.1109/ECCE.2010.5617873.

[10] D.M. Ionel et al., "On the variation with flux and frequency of the core loss coefficients in electrical machines," *IEEE Trans. Ind. Electron.*, vol.42, no.3, pp.658,667, May-June 2006.

[11] T.L. Mthombeni and P. Pillay, "Physical Basis for the Variation of Lamination Core Loss Coefficients as a Function of Frequency and Flux Density," in IEEE Industrial Electronics, IECON 2006 - 32nd Annual Conference on, doi:10.1109/IECON.2006.347545.

[12] A.R. Tariq et al., "Iron and Magnet Losses and Torque Calculation of Interior Permanent Magnet Synchronous Machines Using Magnetic Equivalent Circuit," *IEEE Trans. Magn.,* on , vol.46, no.12, pp.4073,4080, Dec. 2010.

[13] Wooyoung Choi et al., "Core loss estimation of high speed electric machines: An assessment," in IEEE Industrial Electronics, IECON 2006 - 32nd Annual Conference on, doi: 10.1109/IECON.2013.6699556.

[14] R.Dutta and M.F. Rahman, "Comparison of Core Loss Prediction Methods for the Interior Permanent Magnet Machine," in Power Electronics and Drives Systems, 2005. PEDS 2005. International Conference on, doi: 10.1109/PEDS.2005.1619907.

[15] Lei Ma et al., "Prediction of iron loss in rotating machines with rotational loss included," *IEEE Trans. Magn.,*, vol.39, no.4, pp.2036,2041, July 2003.

[16] K. Roy et al, "An online core loss estimation technique for self-excited induction generator," in Power Electronics, Drives and Energy Systems (PEDES) 2010 Power India, 2010 Joint International Conference on, doi: 10.1109/PEDES.2010.5712494.

[17] T. Abbasian et al., "Improved adaptive feedback linearization control of induction motors based on online estimation of core loss and rotor resistance," in Power Electronics, Electrical Drives, Automation and Motion, 2006. SPEEDAM 2006. International Symposium on, vol., doi: 10.1109/SPEEDAM.2006.1649739.

[18] JSOL Corporation, JMAG, Chuo-Ku, Tokyo, Japan, 2013, [online], Available: http://www.jmag-international.com/.